Spring 5-6-2019

FATE MAP OF THE BLASTODERM TO DETERMINE SEGMENTAL FATE IN TRIBOLIUM CASTANEUM

Latanya Coke
latanyacoke@gmail.com

TRINITY COLLEGE

FATE MAP OF THE BLASTODERM TO DETERMINE SEGMENTAL FATE IN *TRIBOLIUM CASTANEUM*

BY

LATANYA N. COKE

A THESIS SUBMITTED TO
THE FACULTY OF THE DEPARTMENT OF BIOLOGY
IN CANDIDACY FOR THE BACCALAUREATE DEGREE
WITH HONORS IN BIOLOGY

DEPARTMENT OF BIOLOGY

HARTFORD, CONNECTICUT

6 MAY 2019

FATE MAP OF THE BLASTODERM TO DETERMINE SEGMENTAL FATE IN *TRIBOLIUM CASTANEUM*

BY

LATANYA COKE

Honors Thesis Committee

Approved:

_____
Terri A. Williams, Advisor

_____
Robert J. Fleming

_____
Hebe M. Guardiola-Diaz

Date: _____

Table of Contents

Abstract

Segmentation in arthropods has been modeled on the well-defined segmentation patterns found in *Drosophila*. In *Drosophila*, segments form simultaneously in the blastoderm where morphogenic gradients spanning the AP axis provide patterning inputs. However, in most arthropods, segments form sequentially from a posterior growth zone. Sequential segmentation in arthropods has recently been demonstrated to use a vertebrate-like segmentation clock (Sarrazin et al. 2012). The vertebrate segmentation clock is a molecular oscillator that regulates periodic somite formation (Gibb 2010). In the red flour beetle, *Tribolium castaneum*, the segmentation clock is coordinated by traveling waves of expression generated by a pair-rule gene oscillator. For this study, we aimed to identify and describe regulatory controls of the *Tribolium* clock and construct a fate map of the blastoderm. We particularly focus on whether the output of the clock at the blastoderm stage - prior to the striking rearrangements of germband formation - actually determines cell fate. From preliminary studies we know that the *caudal* and *even-skipped* genes are two key genes of the *Tribolium* segmental clock. To understand how the clock is regulated, we identified and isolated 2 kb upstream of the *caudal* promoter region. We have cloned and sequenced this fragment to use in building reporter constructs that will be used to identify the cis-regulatory region driving wild type *caudal* expression. A deletion series of those regions showing enhancer activity will be completed to resolve the cis-regulatory regions to smaller domains (~500 bp-1.5 kb). In efforts to generate a fate map of the blastoderm, we created the T3-Nls-Eos DNA template for later mRNA synthesis. We will perform embryo injections with mRNA encoding for EosFP to determine the degree to which segmental fate is determined at the blastoderm stage of developmental.

Introduction

Segmentation, the division of an organism's body into a series of repeated units, is widespread in the animal kingdom. The three major taxa that demonstrate segmented body plans - Arthropoda, Chordata, and Annelida - are highly diverse. The arthropods are the most speciose phylum on earth and display outstanding diversity in adult morphology (Fortey and Thomas 1997). There are four major classes within Arthropoda, the largest of which is the Insecta. The insect adult body plan is extremely well conserved. Regardless of differing developmental strategies, all adult insect bodies consist of a head (six segments), a thorax (three segments), and an abdomen (eight to 11 segments) (Liu and Kaufman 2005). Yet, surprisingly, where they are known, the developmental mechanisms of segmentation that produce that conserved adult body plan are highly variable.

The great diversity of early insect development has been categorized into three types: short, intermediate, and long germband (where germband refers to the elongated, segmented embryo). Traditionally, the length of the embryonic rudiment, the first visible sign of the developing body, is used for classifying embryos (Davis and Patel 2002). In long germband insects, the embryonic rudiment takes up virtually the entire length of the egg. By contrast, the embryonic rudiment in short germband insects occupies only a small area of the anteroposterior axis of the egg, while the remaining area develops into extraembryonic tissue, the amnion and serosal layers. The short-intermediate-long germband classifications have long been expected to be correlated with developmental mechanisms generating the segmented body (Sander 1994; Tautz et al 1994). While it is easy to measure the length of the embryonic rudiment, classifying an embryo as either short, intermediate, or long often implies combinations of other characteristics. These characteristics include segment

patterning on the blastoderm and degree of posterior cell proliferation, both of which are difficult to measure (Williams and Nagy, 2017; Nagy and Williams, in prep).

Decades of work have been dedicated to understanding how assumptions based on short-intermediate-long germband categorizations relate to the cellular and molecular processes that govern sequential segmentation in insects (Sander 1994). Nonetheless, the linkage of the two remains unclear, as it is not yet known: 1) when blastoderm cells are committed to their segmental fates, 2) what the contributions of cell division and movement are to embryonic growth, and 3) how 1 and 2 are related to one another. Short and intermediate germband embryos are inclusive of the more basal, hemimetamorphic orders, such as Ephemeroptera and Orthoptera; while long germband embryos are constrained to the more derived metamorphic orders, such as Diptera. Long germband developing embryos, modeled by *Drosophila*, specify all segments simultaneously on the blastoderm and require minimal mitotic contributions (Liu and Kaufman 2005). In contrast, short and intermediate germband developing embryos are assumed to only specify anterior segments on the blastoderm (Davis and Patel 2002, while posterior segments develop sequentially during the germband stage) and have been assumed to require extensive posterior cell proliferation, generating naïve tissue for subsequent patterning (Sander 1996; Williams and Nagy 2016). Unfortunately, our current understanding of the developmental mechanisms that govern sequential segmentation in insects is limited and mainly based on comparisons of segmentation patterns to the well-studied *Drosophila* paradigm.

The work of Nüsslein-Volhard and Wieschaus (1980) pioneered our understanding of the molecular basis of segmentation in *Drosophila*. In *Drosophila,* a hierarchy of gene

regulation is used to build the anterior-posterior[1] body plan, specifically, the maternal effect genes, gap genes, pair-rule genes, and segment polarity genes (Gilbert 2000). These genes progressively subdivide the embryo into all 14 segments[1] of the adult. The developing embryo is initially patterned by maternal effect genes from mRNAs differentially localized in the egg. Those mRNAs encode regulatory proteins used to activate or repress the expression of specific zygotic genes, called gap genes. Mutations in gap genes cause gaps in the segmentation pattern. Gap genes encode for transcription factors that regulate the transcription of pair-rule genes. The pair-rule genes are responsible for a transitory double segment organization of the embryo. There are seven pair-rule stripes expressed on the blastoderm (Gilbert and Barresi 2016). Transcription factors encoded by pair-rule genes activate the segment polarity genes, responsible for dividing the embryo into fourteen segments. The seven pair-rule stripes on the blastoderm corresponds to three mandibular, three thoracic and eight abdominal segments formed later in development (Akam 1987). In *Drosophila*, the fate of blastoderm cells support the assumptions made for long germband embryos. UV irradiation experiments in *Drosophila* demonstrated a direct relationship between the location of larval epidermis defects and the position of irritation on the blastoderm (Lohs-Schardin et al., 1979; Hartenstein and Campos-Ortega, 2014). Furthermore, the expression pattern of the pair-rule genes is a direct molecular marker of the blastoderm fate map (Tautz et al. 1994).

Although simultaneous morphological segmentation, germband length, and segmental patterning on the blastoderm correlate as expected in the *Drosophila* embryo,

[1] *Drosophila* diverges from the conserved insect adult body plan on account of their poorly define gnathal (head) segments. The condensed pre-gnathal segments are counted as one segment (Schmidt-Ott et al. 1994).

there is mixed evidence to support these features being coupled in other insect species. Moreover, simultaneous patterning of segments in *Drosophila* is a derived mode of segmentation (Damen 2007). In most other insects, segments are formed sequentially from a posterior growth zone. Because of this, *Drosophila* is not an ideal model for segmentation in all insects and whether the blastoderm patterning is a predictor of fate is unclear in most insects.

Vertebrate-like Segmentation clock in Arthropods

Sequential segmentation is not unique to the Insecta, most segmented animal species develop their segments sequentially. In vertebrates, sequential segmentation is regulated by a "segmentation clock" in the growth zone (Pourquie 2001). The vertebrate segmentation clock is a set of interacting genes whose temporal oscillations regulate periodic somite formation (Palmeirim et al. 1997). While well known in vertebrates, sequential segmentation in arthropods has only recently been hypothesized to use a segmentation clock (reviewed in Liao and Oates 2017), and the presence of a clock has only been experimentally demonstrated in the red flour beetle, *Tribolium castaneum* (Sarrazin et al. 2012). The genes that regulate sequential segmentation in arthropods have been a focus of study for molecular and development biologists in the last 10-15 years. In *T. castaneum*, the segmentation clock is coordinated by traveling waves of expression generated by a pair-rule gene oscillator (El-Sherif et al. 2012). The pair-rule components of the oscillator – *even-skipped* (*Tc-eve*), *odd-skipped* (*Tc-odd*), and *runt* (*Tc-run*) – form a three-gene circuit to regulate one another (Choe et al., 2006). In the proposed model of the pair-rule gene circuit, *Tc-eve* expression activates *Tc-run*, that, in turn, activates *Tc-odd* (see **Figure 1**). Subsequently, *Tc-odd* expression

represses *Tc-eve*, defining a primary *Tc-eve* stripe from the broad expression domain. The pair-rule gene circuit sets up segments sequentially with a double segment periodicity both in the early blastoderm stage and during germband elongation (Choe 2006, El Sherif et al., 2012). The gene of interest, *Tc-eve*, activates *engrailed* which specifies the posterior end of each segment. Thus, the output of the segmentation clock, *even-skipped* expression, leads to segment specification.

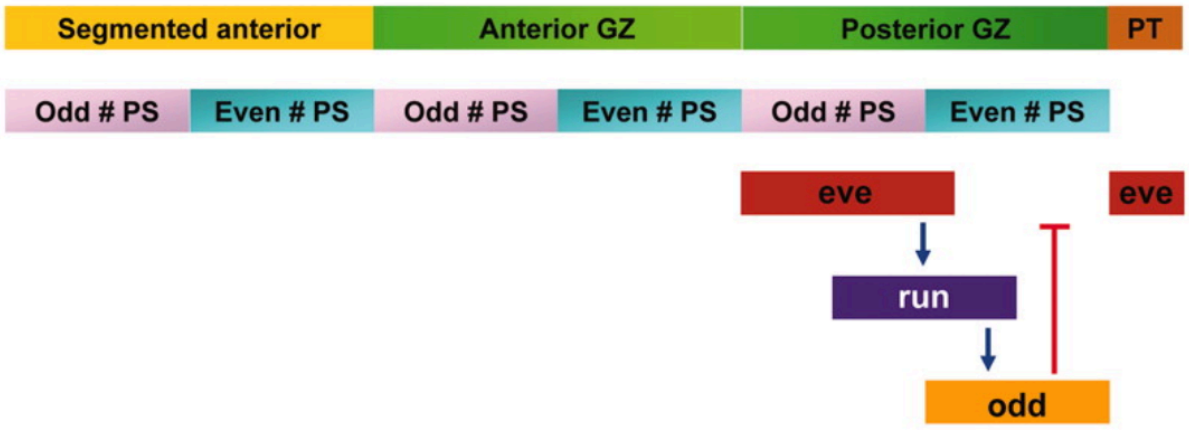

Figure 1: **Summary of the dynamic expression and regulatory interactions of the primary pair-rule genes.** Top bar indicates that posterior is to the right. New segments are added from the posterior growth zone. For each cycle of the gene regulatory circuit (*Tc-eve*, *Tc-run*, and *Tc-odd*) two segments are pre-patterned in the posterior growth zone. *Tc-eve* expression activates *Tc-run*, that, in turn, activates *Tc-odd* which represses *Tc-eve,* completing the circuit. From Choe et al 2006.

The *Tribolium* segmentation clock begins patterning prior to formation of the embryo proper

Segmentation in *Tribolium* occurs sequentially, through the specification of blocks of ectodermal cells within an epithelium. In the early blastoderm stage, the cells are uniform and basally continuous with the yolk sac. However, during embryogenesis there are dramatic cell movements and tissue rearrangements generating a condensed, multilayered embryo (Benton and Pavlopoulos 2014). Specifically, following the formation of the blastoderm (see

Figure 2A), dramatic cellular rearrangements condense cells towards the posterior region (see **Figure 2B**), forming the initial embryo, called the germband, which is surrounded by extraembryonic tissue. After the germband condenses, it continues to lengthen and add segments sequentially in an anterior to posterior progression (see **Figure 2C**). Germband elongation is driven by extensive cellular rearrangements and some cell division. However, the segmentation clock begins patterning prior to the dramatic rearrangements of the embryo before and during germband formation (see **Figure 2B**). More striking, based on examination of fixed embryos (El-Sherif et al. 2012), cells appear to maintain a continuous band of gene expression while undergoing extensive cell movements — creating a challenge in segmental patterning not met in vertebrate segmentation (Nagy and Williams, in prep). In both the blastoderm and germband stages of *Tribolium* development there are continuous waves of *Tc-eve* expression that propagate from posterior to anterior (El-Sherif et al. 2012) (see **Figure 3**). However, it is not unequivocal whether the outputs of the segmentation clock are maintained between the blastoderm and germband stages of *Tribolium* development.

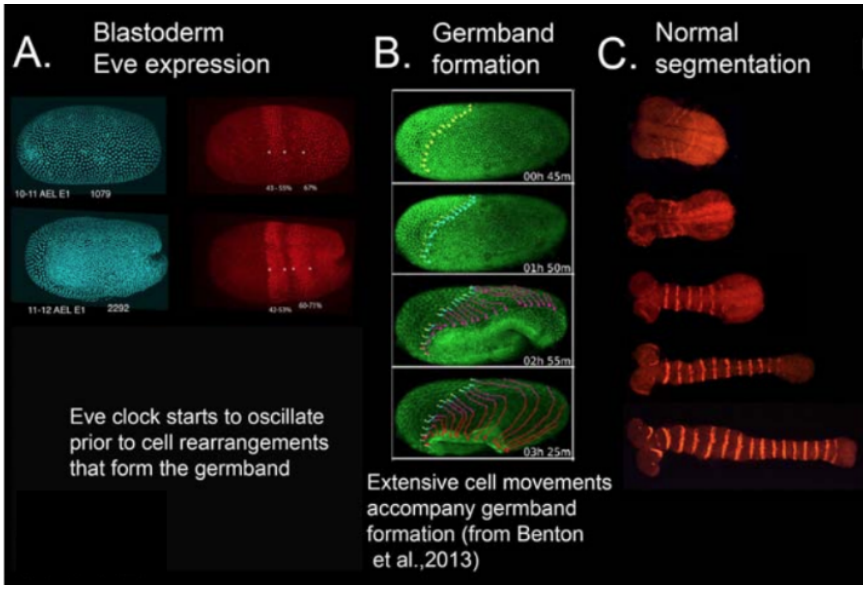

Figure 2: **Outputs of the *Tribolium* Segmentation clock during the blastoderm and germband stages of development.** A. Blastoderm stage (top). Early germband formation (bottom). DAPI nuclear staining in blue (left). *Tc-eve* staining in red (right). The segmentation clock begins in the blastoderm stage prior to the formation of the germband (Nagy lab). B. Lateral view tracking the pattern of cell movement during embryogenesis in wild type *Tribolium* embryos. Purple tracks trace the extreme cell movements that accompany the formation of the early germband (Benton et al., 2013). C. Developing *Tribolium* embryos stained with *engrailed* used to highlight the posterior of each segment. Segments are added sequentially with an anterior to posterior progression (Nakamoto et al 2015).

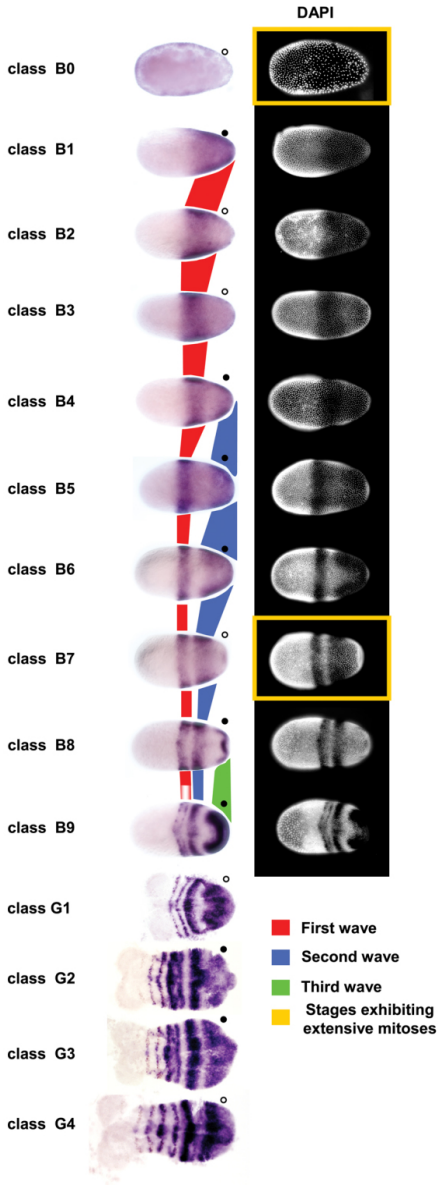

Figure 3: **Tc-*eve* expression appears continuous in fixed stages from the early blastoderm (B0-B9) to early germband (G1-G4) stages of development.** The first Tc-*eve* strip highlighted in red, second in blue, and third in green. Waves of Tc-*eve* expression propagate up the embryo from posterior to anterior. From El Sherif 2012.

In *Drosophila,* the blastoderm fate map represents the complete future body plan. By contrast, the blastoderm is expected to define anterior segments in *Tribolium*. Nakamoto et al. (2015) conducted a study comparing the segmental fates of marked *Tc* blastoderm cells along the anterior/posterior egg axis. The results from that study revealed ambiguities in *Tc*

segment formation. For example, cells at 60% egg length in the early blastoderm produced the second and third thoracic segments, which should be derived from the third pair-rule stripe. Yet, the first appearance of the third pair-rule stripe occurs only at the very posterior end of the embryo, at the formation of the posterior amniotic fold (i.e., quite posterior to 60% egg length). The discrepancies highlighted in Nakamoto et al. (2015) emphasize the rapid posterior movements undergone by blastoderm cells and dynamic nature of the blastoderm. In addition, Nakamoto et al. (2015), demonstrated that in *Tribolium* blastoderm cells at the same egg length ended up in a range of different segments. Finally, they showed that the rate of segment addition varies between early and late segmentation, raising the question of how the clock is differentially regulated at those times. This differential timing of segmentation prompts us to examine the promoters of *caudal* and *eve* for candidate regulators that might account for this change in tempo.

Generating a comprehensive fate map of the blastoderm

As discussed earlier, it is unclear whether the *Tc-eve* stripes seen in the early blastoderm correspond to the germband segments. Do cells on the blastoderm acquire their fate or does that occur after germband formation? Fortunately, a more extensive fate map of the blastoderm could help us to determine to what degree the initial output of the segmentation clock is stably maintained through cell rearrangements. Cell lineage and fate map analysis are fundamental tools for understanding development in animal systems (Brown et al. 2009). The dynamic gene expression patterns of *Tc-eve* detailed above are currently inferred from immunohistochemical preparations of fixed *Tribolium* embryos (see **Figure 3**). However, those expression patterns have yet to be followed in the live rearranging

embryo. The use of a fluorescent photoconvertible protein will allow us to overcome this shortcoming. By photoconverting and tracing cells from the first *Tc-eve* band, we aim to answer: If the first *eve* band on the blastoderm corresponds with the first pair of segments in the germband; or, in general, whether early outputs of the segmentation clock, during the blastoderm stage, specify later germband segments. Moreover, this general fate mapping will be very informative about which cells end up where and to what degree fate is determined at the blastoderm stage.

Materials & Methods

Eos Fluorescent protein and Nuclear localization signal

A gene encoding a fluorescent protein (FP) from *Lobophyllia hemprichii* was cloned in *Escherichia coli* and characterized by biophysical and biochemical methods (Wiedenmann et al. 2004). The protein, EosFP, emits robust green fluorescence (516 nm) and is converted to red fluorescence (581 nm) upon near-ultraviolet irradiation at ≈390 nm. In this study, EosFP is used as tool for *in vivo* monitoring of cell movement during embryogenesis to reveal the fate of the cells from the first segment in the early blastoderm. Our goal was to design an Eos for injection in *Tribolium* embryos and given our starting plasmid, we tested a variety of strategies to meet that goal (see **Figure 4**).

Designing the Eos construct (the template for mRNA Synthesis)

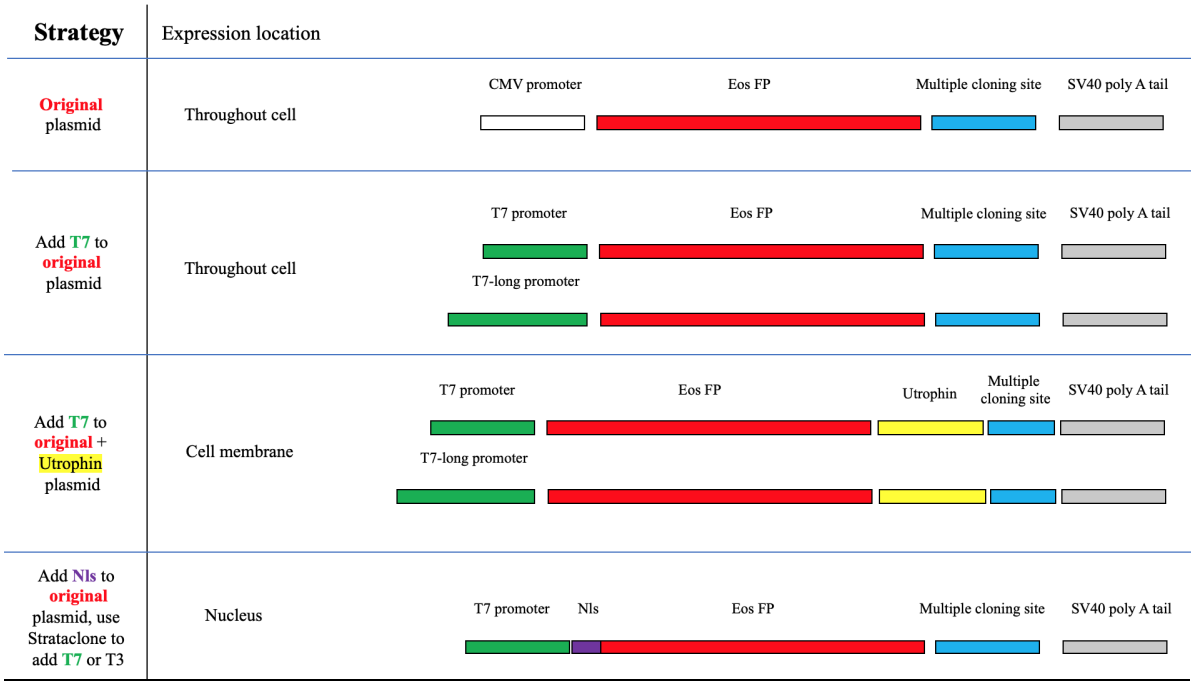

Figure 4: Schematic of the different experimental strategies used to design the Eos construct. The original (mEos3.2) plasmid contains a cytomegalovirus (CMV) promoter used to drive the expression of the EosFP. The multiple cloning site is useful for inserting foreign DNA (Utrophin) into the original plasmid because it contains many unique restriction enzymes sites. The SV40 poly (A) signals the end of transcription. The addition of the T7 (or T3) promoter is required for *in vitro* mRNA synthesis. Utrophin, an actin binding protein, was added to the original plasmid to localize Eos expression to the cell membrane. A nuclear localization signal, Nls, was added to the original plasmid to localize Eos to the nucleus. The product was later transformed into a workable T7&T3 promoter vector.

Strategy 1: Adding the T7 promoter to the original (mEos3.2) plasmid to permit in vitro mRNA synthesis

The mEos3.2 plasmid (**appendix, image 1**) was acquired from the Nagy Lab, Tucson AZ. The mEos3.2 plasmid was equipped with a CMVd1 promoter, EosFP and SV40 poly (A) tail, but it unfortunately lacked both T3 and T7 promoter sites[2]; either of which can be used

[2] The RNA polymerase promoter sites (T7, T3, or SP6) must be upstream of the template DNA sequence to be transcribed.

for capped mRNA synthesis using the mMessage mMachine kit (Thermofisher). Our first strategy was to design T7 and T7-long [3] primers to add T7 promoter to the mEos3.2 by PCR overhang (**Table 1**).

Strategy 2: Adding the T7 promoter to the Utrophin (mEos3.2-Utr-C1) plasmid to grant mRNA synthesis

The mEos3.2-Utr-C1 plasmid was also acquired from the Nagy lab, Tucson Az. The mEos3.2-Utr-C1 plasmid was constructed from a mEos3.2-C1 plasmid and Utrophin from a RFP-Utr plasmid. Utrophin is an actin binding protein, and thereby attaching Utrophin to the Eos would allow us to visualize cell outlines. By similar methods, we added T7 promoter binding sites to the mEos3.2-Utr-C1 plasmid (**Table 1**).

Table 1: T7 and T7-long overhang primers designed to add T7 promoter sites to the mEos3.2 plasmid and mEos3.2-Utr-C1by PCR.

	Forward primer	*Reverse primer*
T7	5'-taatacgactcactatagggtagtgaaccgtcagatcc-3'	5'-tttgccgatttcggcctattgg-3'
T7-long	5'-gaatttaatacgactcactatagggtagtgaaccgtcagatcc-3'	5'-tttgccgatttcggcctattgg-3'

Forward and reverse sequences of the T7 and T7 long overhang primers. The addition T7 promoter is required for mRNA synthesis.

[3] The T7-long primers were later included as it was shown that increasing A-T sequences upstream of the promoter increased the binding affinity of the RNA polymerase-promoter complex (Tang et al. 2005).

Strategy 3: Adding a nuclear localization signal to the original (mEos3.2) and transferring the product into a workable T7&T3 promoter vector

Using sequencing based on a putative *Tribolium* Nls (5'-PQKRSRN-3' (Wang et al. 2008)), Nls primers were designed to add a nuclear localization signal (Nls) to the mEos3.2 by overhang (**Table 2**). The Eos-Nls PCR product was cloned into the pSC-A vector (see **Figure 3**) using TA cloning (Strataclone, Agilent Technologies). The pSC-A vector was chosen specifically because it contained both T3 and T7 promoter binding sites. The transformed Strataclone cells were plated onto amp/kan agar plates. Three strategies were used to confirm that we had the correct product insert: 1) for the correct size prediction, we conducted a colony PCR, using M13 forward and reverse primers 2) for the correct insert orientation, we conducted restriction enzyme digests using *Eco*RV (see **Figure 5** and **3**) for the final product verification, samples were sent out to Genewiz for Sanger sequencing.

Table 2: Nls overhang primers designed to add the nuclear localization signal to the mEos3.2

	Forward primer	*Reverse primer*
Nls	5'-ccaaagaagaagcgtaaggtaatgagtgcgattaagccag-3'	5'-tttcgctttcttcccttcct-3'

Forward and reverse primer sequences for the nuclear localization signal. Addition of the Nls localizes Eos expression in the cell nucleus.

Figure 5: **Generic map of the StrataClone PCR cloning vector pSC-A-amp/kan**. The pSC-A-amp/kan vector contains both T3 and T7 primer binding sites. PCR product insert site highlighted by grey box. (StrataClone Manual)

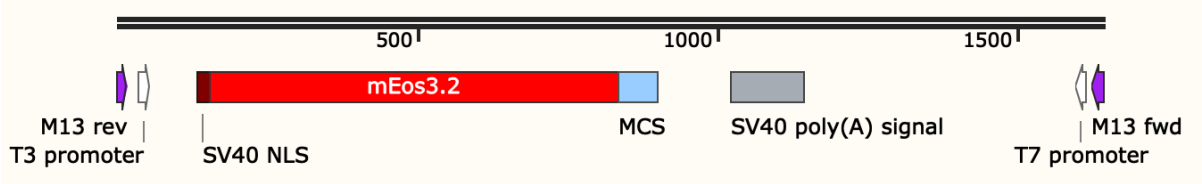

Figure 6**: Eos inserted as a PCR product into pSC-A-amp/kan vector.** Sequence map of 1641 bp putative Nls-Eos- SV40 poly(A) tail oriented in line with the M13 reverse primer and suitable for T3 promoter. Our PCR product inserted in the other direction could use the T7 promoter.

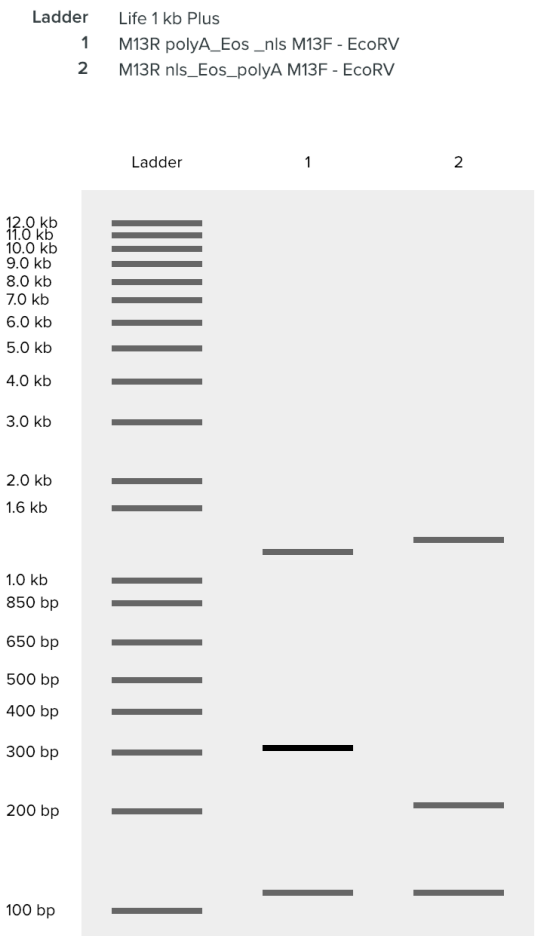

Figure 7: ***Eco*RV digest prediction on 1641 bp product amplified by M13 forward and reverse primers from colony PCR.** Depending on orientation, there is a distinct 200 or 300 bp band corresponding to the T7-Nls-Eos and T3-Nls-Eos (lanes 1 and 2 respectively). The desired orientation was T7-Nls-Eos.

Synthesizing mRNA *in vitro*

Strategy 1: Synthesizing mRNA using the T7-Eos DNA templates

The T7/T7-long and SV40 primers were used to generate linear T7-Eos PCR products. With those pieces of DNA, we attempted to synthesize T7-Eos mRNA using the mMessage mMachine transcription T7 RNA polymerase kit (Thermofisher Scientific).

Strategy 2: Synthesizing mRNA using the T7-Eos-Utr DNA template

The T7/T7-long and SV40 primers were used to generate linear T7-Eos-Utr PCR products. We attempted to synthesize Eos-Utr mRNA using the mMessage mMachine transcription T7 RNA polymerase kit (Thermofisher Scientific).

Study system

We maintain a stock of *Tribolium castaneum* (GA-1 strain, originating from Kansas Stock Center in 2010) in jars of whole wheat flour supplemented with 5% brewer's yeast at 30° C (30-50% humidity). In addition to a fully sequenced genome, *T. castaneum* facilitates genetic analyses with its high fecundity, short life cycle, and ease of culture (Wang et al 2007).

*Tc*Egg lay and collection

To collect eggs for embryo injections, 20 ml of adult beetles were placed into jars containing 200 ml of sieved white flour (number of eggs rely greater on the amount of flour used than number of the female beetles). The adult beetle jars were incubated at 37° C for 1 h. To separate the eggs from adult beetles, clean 700 µm and 300 µm mesh sieves were stacked to allow the 700 µm to catch the adults and the 300 µm to catch the eggs (Beetle book). The eggs were collected into a petri dish and raised at 37° C for an additional 4 h.

Dechorionation

The 4-5 h old eggs were transferred into 0.10 mm mesh egg basket. To remove excess flour, eggs were rinsed with embryo wash (0.7% NaCl, 0.03% Triton) and water. To

dechorionate the embryos, eggs were placed into 5% bleach with agitation for 2 min. Subsequently, eggs were rinsed thoroughly with deionized water until the bleach smell was no longer detectable.

Preparing for Injections

The embryos were transferred with a paintbrush and water to an agar plate with a 100 um mesh placed on top. The embryos were arranged in a line; the posterior pole (pointy-end) oriented to the left. Glass capillary tubes (1.0 outside diameter and 0.75 inside diameter) were used to pull embryo injection needles (Program: heat = 320, pull = 244, velocity = 244, delay = 10).

Embryo injections and live imaging

To optimize our injection conditions, we microinjected capped mRNA encoding for RFP-Utr into pre-blastoderm embryos. To fill the injection needles, the unsharpened ends were dipped into an mRNA, fast green solution (2 ul mRNA, 0.5 ul of 5% fast green). The filled needles were inserted perpendicular to the lateral side of the eggs. A pico spitzer was used to deliver <1 ul of the solution into the embryos (World Precision Instruments pneumatic picopump). Following injections at room temperature, embryos were incubated at 37° C to allow the RFP signal to develop (~2 h). At the uniform blastoderm stage we began long-term confocal live imaging and continued throughout the period of germband extension.

Cloning the putative *caudal* promoter

As part of our larger goal to understand how the segmentation clock is regulated at different stages of segmentation in *Tribolium*, we characterized the promoter regions of *caudal*. An ensembl search of the *Tribolium* genome was conducted for the *caudal* gene. To identify the possible promoter region of the *caudal* gene, primers were designed to target a sequence 2 kb upstream from the start codon (**Table 3**). Dodecyl trimethylammonium bromide (DTAP) DNA precipitation protocol was used to extract genomic DNA from a sample of 10 larvae. To amplify the desired promoter region, we conducted a PCR on the genomic DNA using previously designed forward and reverse primers. Gel electrophoresis was used to confirm the band size of desired PCR product. StrataClone Cloning Kit was used to clone the PCR product. To ensure that the vectors contained the correct product, sequence analysis and colony PCR were conducted.

Table 3: *Caudal* primers designed to target 2 kb portion of the *caudal* promoter

	Forward primer	*Reverse primer*
caudal TR	5'-agacctcttcgaagctgaaaca-3'	5'-cccggactcgacatttcact-3'
caudal BR	5'-agacctcttcgaagctgaaaca-3'	5'-cacttgcgtctgaatctgcg-3
caudal LR	5'-agacctcttcgaagctgaaaca-3'	5'-tctgcggcgataaattccca-3'

Forward and reverse primer putative *caudal* promoter sequences. The *caudal* TR, BR and LR share a common forward primer. Differing reverse primers amplify different ~2kb regions.

Results

Creation of the Eos DNA template for later mRNA synthesis

Beginning with a vertebrate plasmid containing the EosFP (mEos3.2), we attempted to engineer template DNA to synthesize mRNA *in vitro* that would be injected into embryos. For successful mRNA synthesis, our template needed either T7 or T3 promoter sites. We either inserted Utrophin coding regions or added the Nls coding regions to localize the EosFP expressed protein in the cell membrane or nucleus respectively.

Strategy 1&2

We successfully added the T7 promoter to the original mEos3.2 plasmid (see **Figure 8**) generating 1011 bp (T7-Eos) and 1016 bp (T7-long-Eos) products. We also added the T7 promoter to the mEos3.2-Utr-C1 plasmid (not shown) generating 1926 bp (T7-Eos-Utr) and 1931 bp (T7-long-Eos-Utr) products. After sequencing results confirmed the presence of the T7 promoter, we continued by attempting to generate mRNA from the constructs. We failed to synthesize mRNA from either the T7-Eos, T7-long-Eos, T7-Eos-Utr, or T7-long-Eos-Utr DNA templates (see **Figure 9**, **Table 4**). We were able to synthesize mRNA using the positive control template included in the kit (*Xenopus* elongation factor 1α, pTRI Xef). But, in a mixing experiment (see **Figure 9**) synthesis of the positive control was inhibited by the presence of the EosFP containing templates; no mRNA was synthesized.

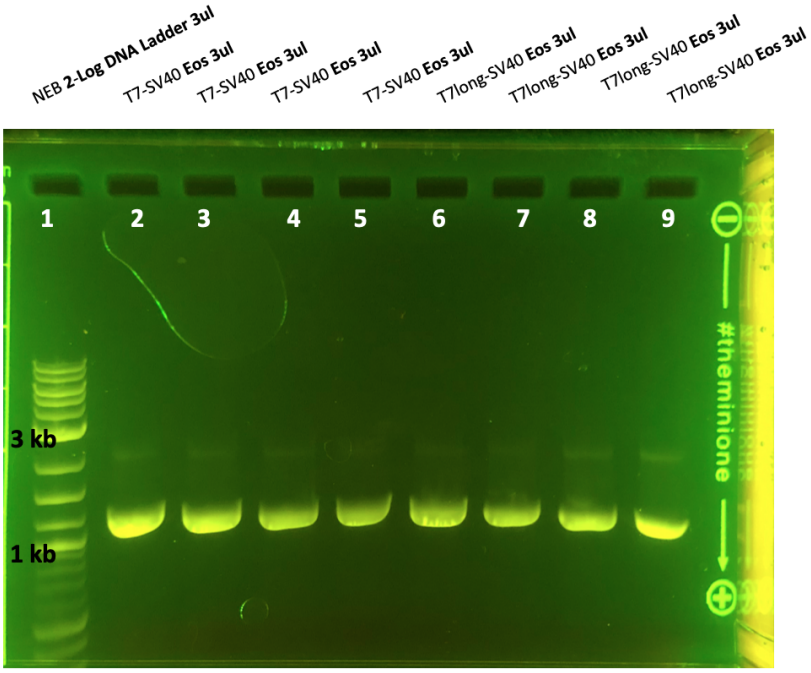

Figure 8: **PCR analysis to confirm the addition of T7 primer binding sites to the mEos3.2 plasmid using forward T7 and T7-long overhang and reverse SV40 primers**. The expected product size for the T7 was 1011 bp. The expected product size for the T7-long was 1016 bp. The expected sizes were approximately recovered in lanes 2-9. No positive or negative control. Gel conditions: miniOne 1% TBE green kit 40 minutes.

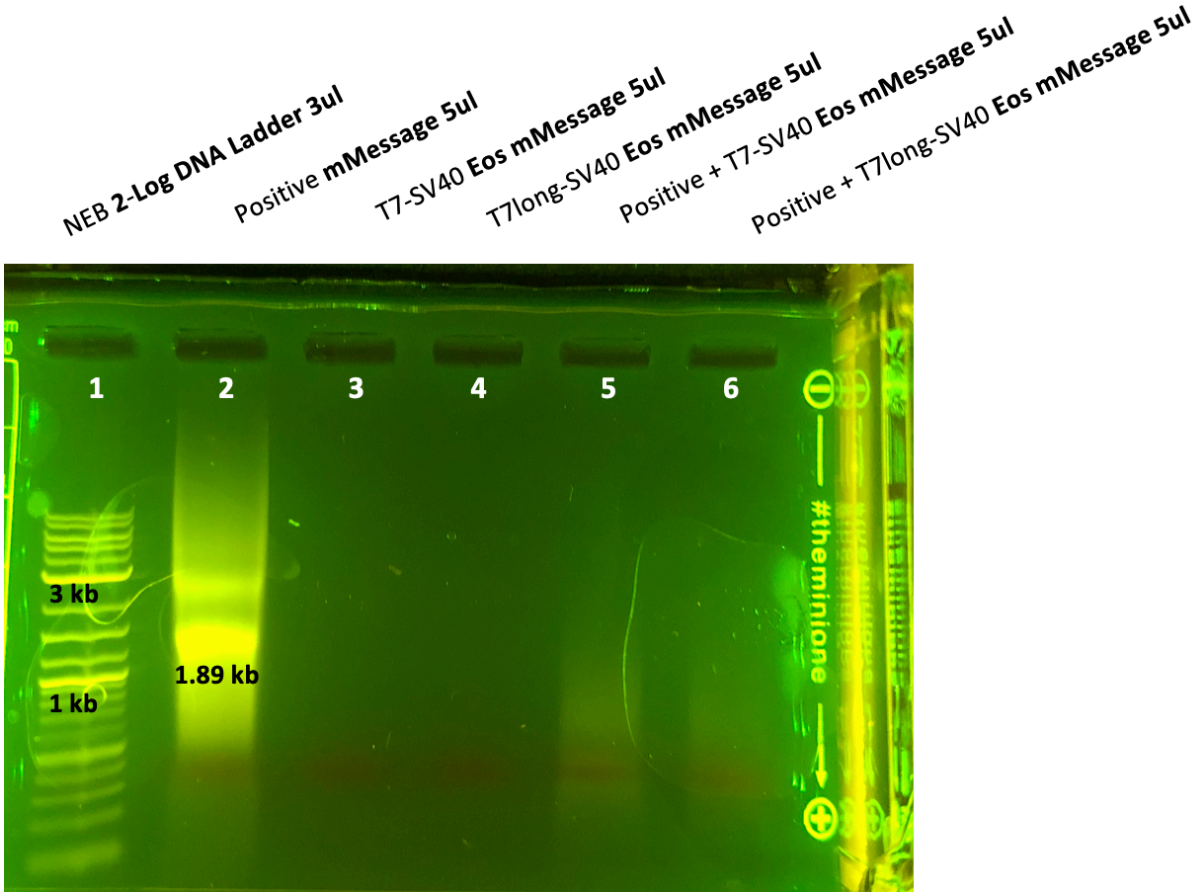

Figure 9: **mMessage mMachine T7 transcription of EosFP, mixing experiment.** Lane 2 = control template DNA. Lanes 3&4 = experimental template DNA. Lane 5&6 = control and experimental template DNA. Control template DNA is inhibited by the presence of experimental template. 100 ng of template per lane.

Table 4: Summary of the results of the different experimental strategies used to design the EosFP construct for embryo injections

Strategy	Gel verification	Sequence verification	mRNA synthesis
Original Plasmid	No	No	No
Add T7 to original Plasmid	Yes: Figure 8	Yes	Unsuccessful
Add T7 to original + Utrophin plasmid	Yes	Yes	Unsuccessful
Add Nls to original plasmids, use StrataClone to add T3	Yes: Figure 10, 12	Yes	Not yet

Successfully added T7 promoter to the mEos3.2 and mEos3.2-Utr plasmids. Failed to synthesize mRNA from either the T7-Eos or T7-Eos-Utr template DNA. Successfully added Nls to mEos3.2 and transformed Nls-Eos product into a StrataClone vector generating T3-Nls-Eos.

Strategy 3

After failing to synthesize mRNA from the constructs generated from strategies 1&2 and failure to confirm that we had the correct Utrophin insert, we designed a new construct. We added the nuclear localization signal to the mEos3.2 plasmid by PCR overhang thereby generating a 1381 bp (Nls-Eos) product. **Figure 10** shows the gel verification that the Nls was added. As a positive control, we used the forward T7 primer and reverse S4V0 to amplify a known 1000 bp (T7-Eos) product. Although a weak band appears in the negative control (T7 and SV40 primers only) it doesn't appear in our other samples and was ignored as an artifact. Proceeding, we transformed the Nls-Eos PCR product into a pSC-A vector. As seen in **Figure 11**, colony PCR gel verification confirmed that the insert was a 1641 bp product. Restriction enzyme digestion analysis predicted that all of our clones were in the T3 orientation. Sequencing analysis verified that our product was in the T3 orientation and not our initially desired T7 orientation (**Table 4**).

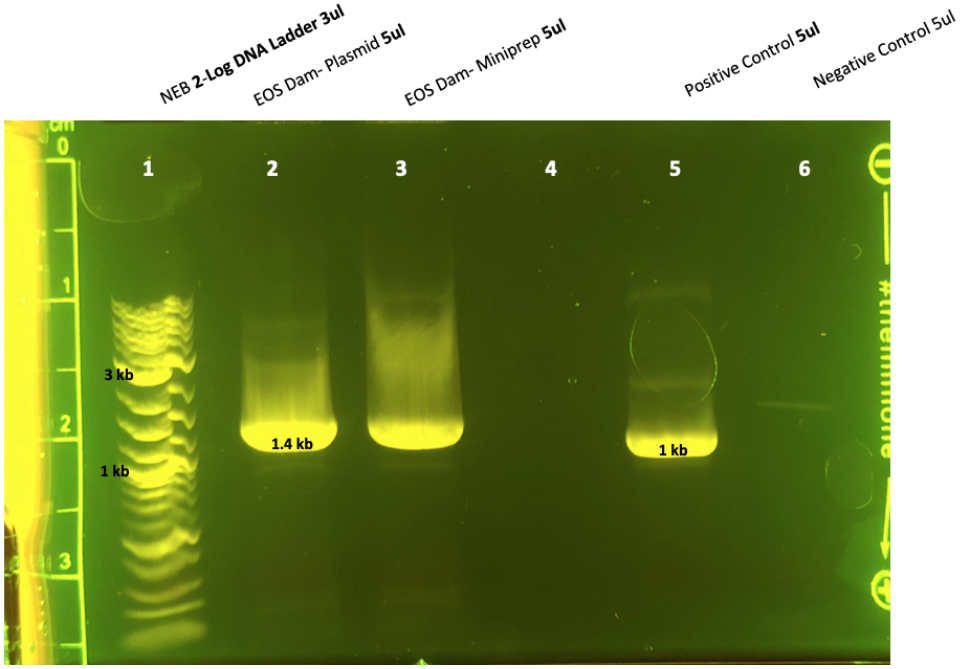

Figure 10: **PCR analysis to confirm the addition of Nls overhang to the mEos3.2 plasmid using Nls-overhang primers**. Both samples, plasmid DNA and miniprep, produce an expected band at 1381bp. Forward T7 and Reverse SV40 primers used as positive control. Gel conditions: ran miniOne 1% TBE green kit for 35 minutes.

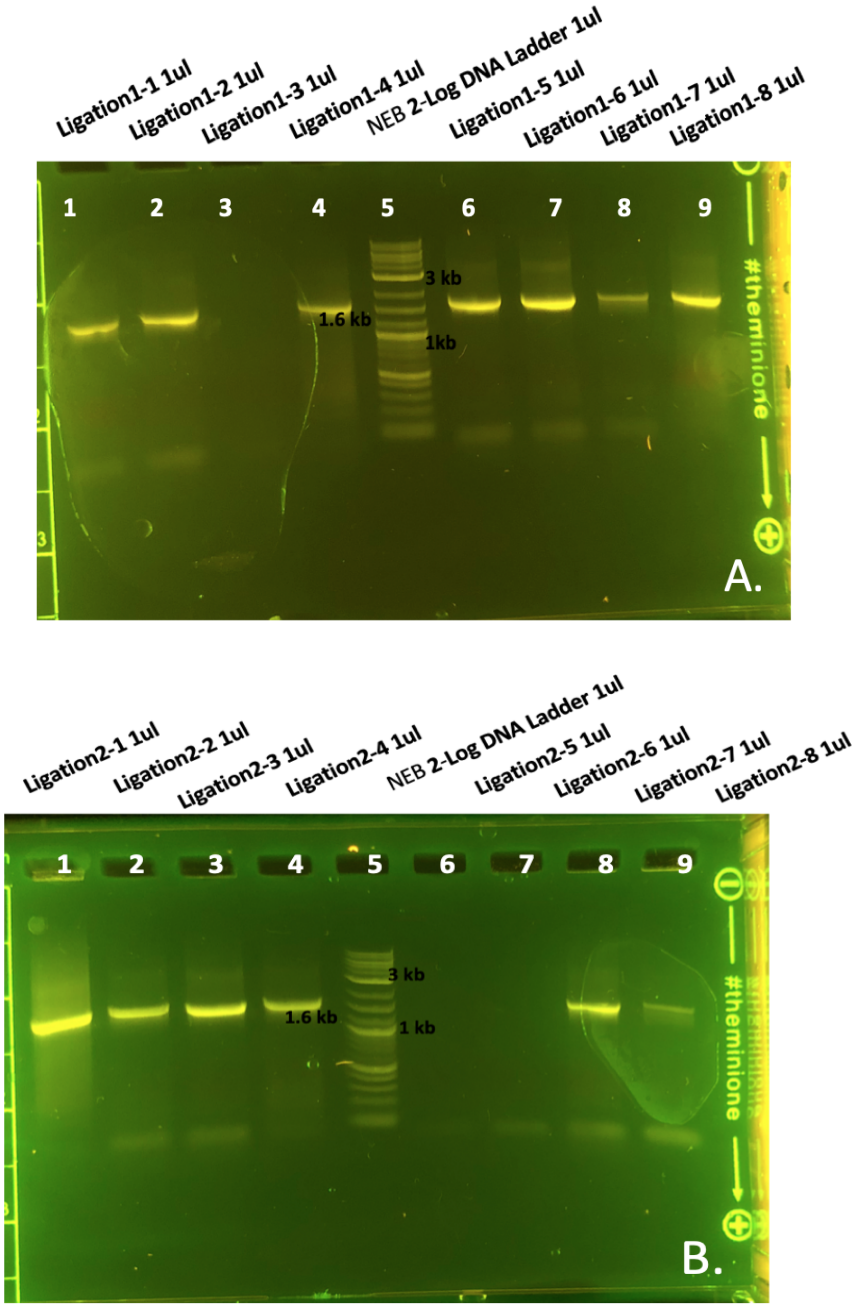

Figure 11: **Colony PCR gel verification using M13 forward and reverse primers.** A) Ligation 1 = Eos Dam- plasmid B) Ligation 2 = Eos Dam- miniprep. The insert, Nls-Eos product, produce an expected band at 1641bp. Gel conditions: ran miniOne 1% TBE green kit for 20 minutes.

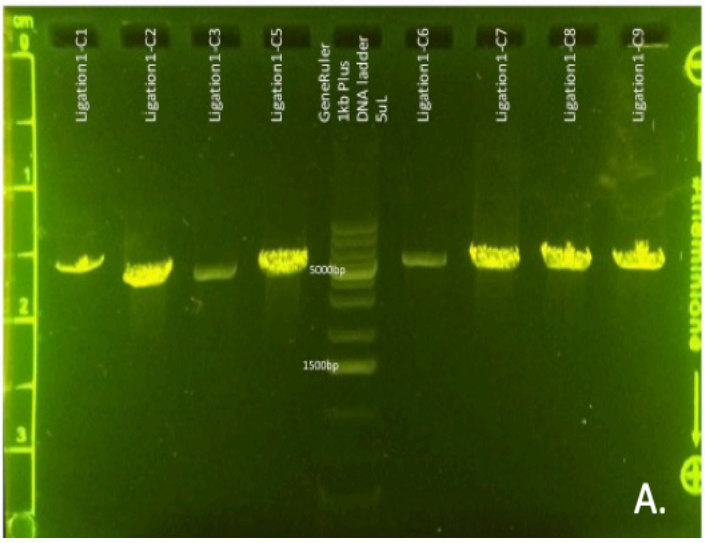
Ligation1-C1
Ligation1-C2
Ligation1-C3
Ligation1-C5
GeneRuler 1kb Plus DNA ladder 5uL
Ligation1-C6
Ligation1-C7
Ligation1-C8
Ligation1-C9
5000bp
1500bp
A.

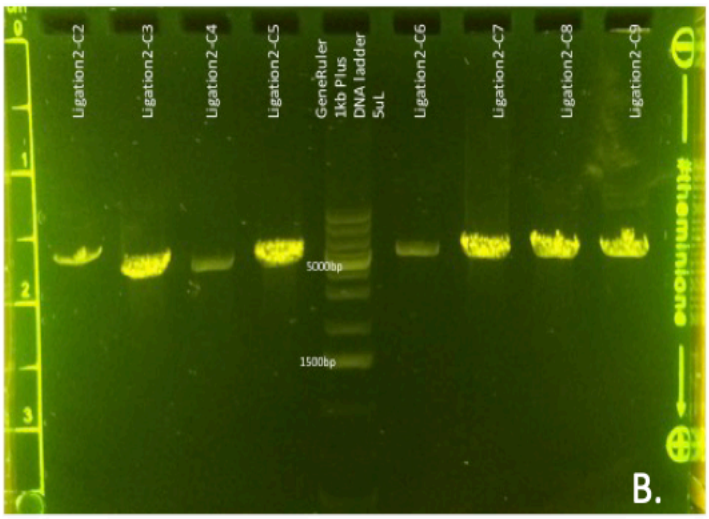
Ligation2-C2
Ligation2-C3
Ligation2-C4
Ligation2-C5
GeneRuler 1kb Plus DNA ladder 5uL
Ligation2-C6
Ligation2-C7
Ligation2-C8
Ligation2-C9
5000bp
1500bp
B.

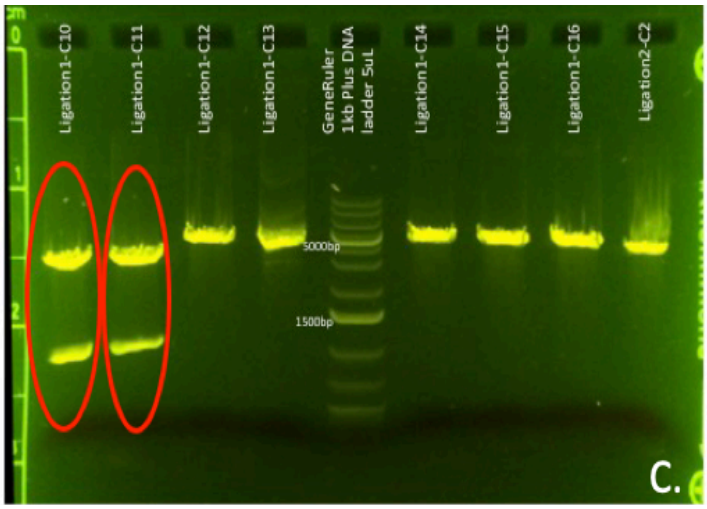
Ligation1-C10
Ligation1-C11
Ligation1-C12
Ligation1-C13
GeneRuler 1kb Plus DNA ladder 5uL
Ligation1-C14
Ligation1-C15
Ligation1-C16
Ligation2-C2
5000bp
1500bp
C.

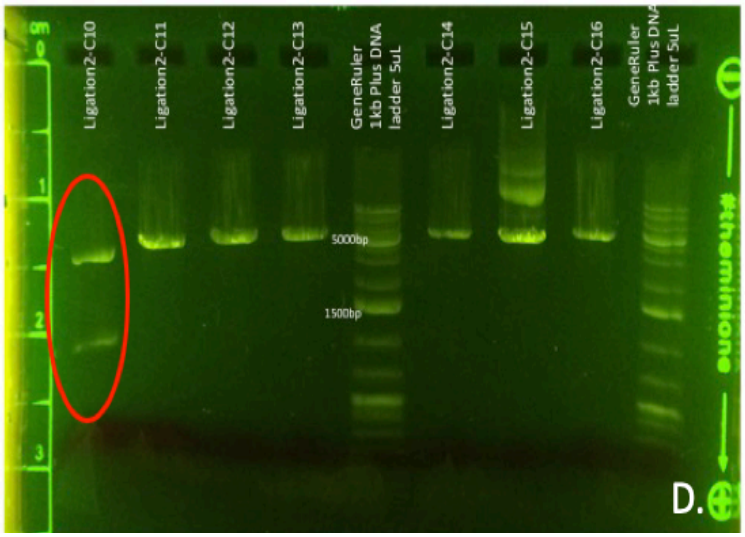

Figure 12: **Restriction enzyme digests using *Eco*RV to confirm insert orientation on 1641 bp product amplified by M13 forward and reverse primers from colony PCR.** A and C) Ligation 1 (Eos Dam- plasmid); B and D) Ligation 2 (Eos Dam- miniprep). Circled clones in red correspond to prediction 2 (see appendix, image 2) that is indicative of the T3 orientation.

Cloning of the putative *caudal* promoter region

To investigate the differential regulation of the segmentation clock, we successfully cloned a 2 kb portion of the putative caudal promoter. **Figure 13** shows the amplification of genomic DNA using our designed *caudal* promoter primers. The *caudal* TR and *caudal* BR samples were observed at the expected 2 kb and therefore were chosen for colony PCR gel verification. **Figure 14** shows the colony PCR gel verification which supports that we have the correct vector insert correct size for: TR *caudal* 2-7 and BR *caudal* 1-4, 6-8. Sequence analysis confirmed the correct sequence for: TR *caudal* 6, BR *caudal* 3, BR *caudal* 7.

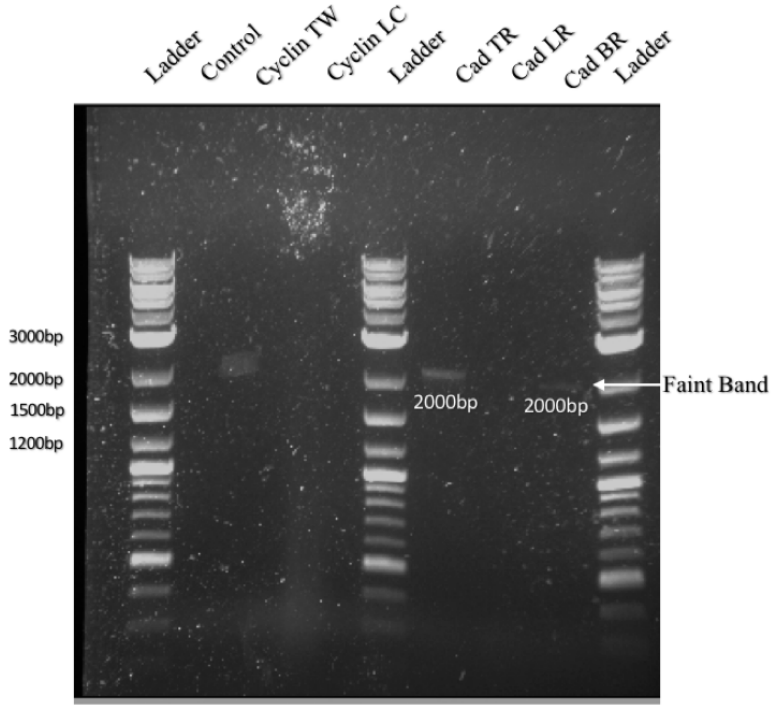

Figure 13: **PCR analysis of extracted genomic DNA using *caudal* TR, *caudal* LR *caudal* BR primers.** Cyclin TW and cyclin LC primers used as negative control. Expected 2 kb band observed for *caudal* TR and *caudal* BR primers.

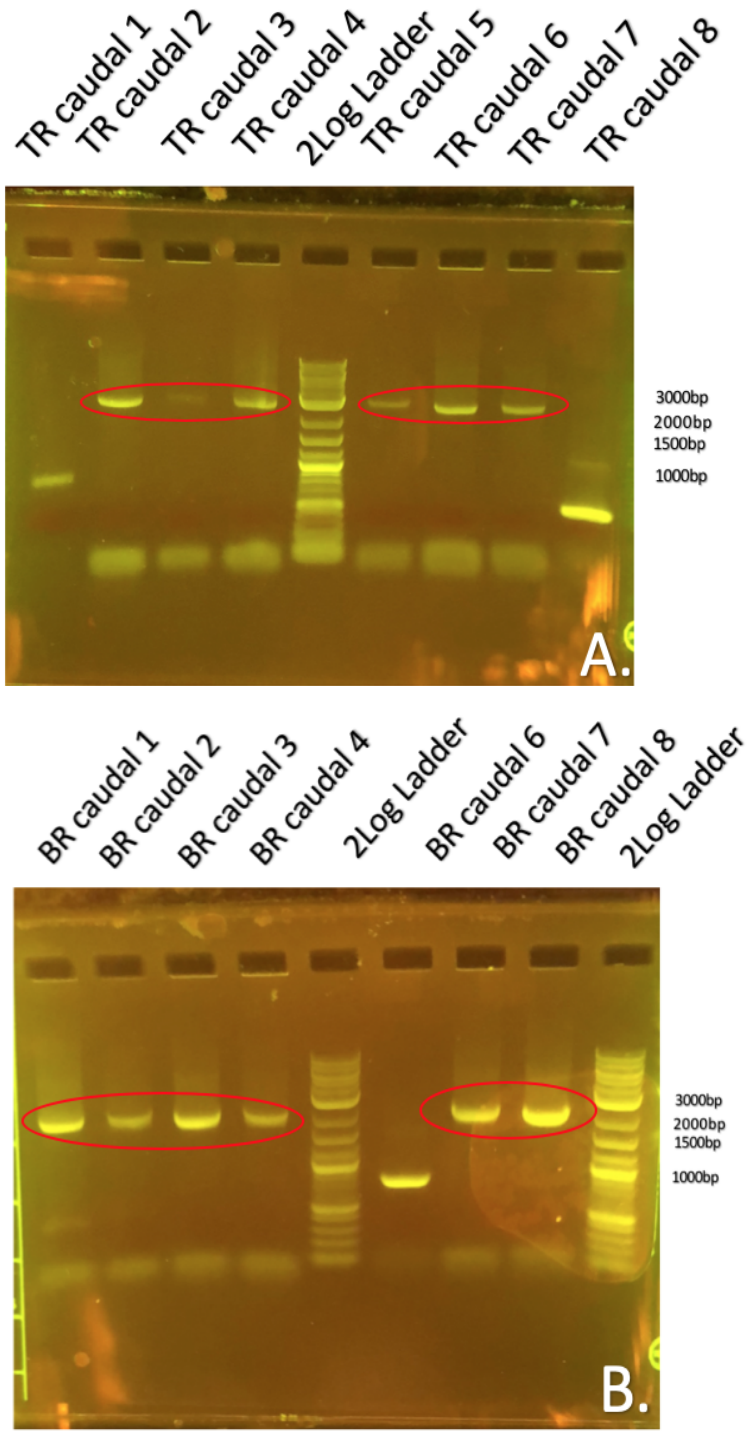

Figure 14: A) ***caudal* TR colony PCR gel verification using M13 forward and reverse primers.** All samples, with the exception of TR *caudal* 1 and TR *caudal* 8 were observed at the expected 2 kb band size. B) ***caudal* BR colony PCR gel verification using M13 forward and reverse primers.** With the exception of BR *caudal* 6, all samples were observed at the expected 2 kb band size.

Discussion

For this study, we attempted to generate a comprehensive fate map of the blastoderm, using intracellular injection of a fluorescent photoconvertible protein in combination with live cell imaging, to investigate whether the early gene expression patterns of a cell represented its later segmental fates. Assuming that the initial length of germband is strongly coupled with the number of segments specified on the blastoderm, we expected the segmental fate maps of sequentially segmenting insects, short and intermediate germband, would differ from the segmental fate map of *Drosophila*, a long germband insect. From previous studies, we assumed that cells in the posterior of the blastoderm would give rise to more segments than those more anterior (Nakamoto et al 2015). Ultimately, by generating a fate map of the blastoderm, we hoped to learn more about of the roles of cell and tissue rearrangement in shaping the embryo and patterns of genes expression at specific times during embryo development.

As detailed below, the creation of our fate map was slowed by unsuccessful attempts to synthesize mRNA encoding for the Eos fluorescent photoconvertible protein. However, we have produced a Nls-Eos with a T3 promoter that will be tested for this purpose moving forward.

Strategy 1&2: Adding T7 promoter to mEos3.2 or mEos3.2-Utr

Although the Eos fluorescent photoconvertible protein has no specific localization in the cell, we thought it would be quickest method to add the T7 promoter to the mEos3.2 vector upstream of the Eos sequence to be transcribed. In adding the T7 promoter we

followed Tang et al., (2005) who found that having a longer T7 region increased transcription. But we found that having a longer T7 region had no effect on transcription.

Our mEos3.2-Utr was designed based on a RFP-Utr that had been used previously to successfully synthesize mRNA. Including the Utrophin would allow us to localize Eos protein expression in the cell membrane. We successfully added the T7 promoter to both mEos3.2 and mEos3.2-Utr vectors, generating T7-mEos3.2 and T7-mEos3.2-Utr products. However, neither product successfully synthesized mRNA. A mixing experiment, of control and experimental templates, suggested that there were inhibitors present in the DNA template preventing transcription.

Strategy 3: Put Nls-mEos3.2 into a T7 Vector

Because our T7-mEos3.2 and T7-mEos3.2-Utr constructs failed to make mRNA, we decided instead to add a nuclear location localization signal to the Eos sequences before using cloning to add the T7 or T3 promoter. By doing so we could localize Eos expression to the nucleus which is best for filming. We transformed the Nls-mEos3.2 into a pSC-A vector specifically because it contained both T3 and T7 promoters. Because TA cloning is not directional, we expected our product from our initial transformation to be inserted in the sense and antisense directions with equal probability. Surprisingly, we found most of our inserts were oriented in the antisense direction. The sense orientation, with the T7 promoter upstream of the sequence, was our preferred orientation and thus, we dedicated our efforts to finding T7 clones. We originally chose the T7 polymerase over the T3 on account of its greater efficiency and higher yield (we needed 2-3 ug/ul of mRNA for embryo injections; Golomb and Chamberlin 1977; Klement et al. 1990). Restriction enzyme digestion was a

helpful tool to differentiate the insert orientation. Using *Eco*RV we could distinguish T7 from T3 clones by looking at different the expected band patterns. In the interest of time, we ordered the T3 polymerase kit to move forward with our sequenced, confirmed T3-Nls-Eos products.

With our T3-Nls-Eos products, our next steps are to synthesize mRNA and perform embryo injections. We have already optimized the embryo injection needles and injection/post-injection survival conditions. Embryos were injected with mRNA encoding for RFP-Utr and survived live confocal imaging from the blastoderm stage to germband stage of development. However, before we can proceed to generating a fate map, we must first determine how long it takes for Eos expression to develop and how to uniformly photoconvert cells.

In general, the output of the segmentation clock regulates the timing of segment formation. Whereas the vertebrate segmentation clock has species-specific rates of segment addition, the *Tribolium* segmentation clock has variable phases of segment addition (Nakamoto et al 2015). Our 2kb caudal promoter fragment is being used to investigate the regulatory control of differential timing. We successfully cloned 2kb of the putative promoter region of the *caudal* gene. Our next steps include using pieces of our promoter region to create a series of reporter constructs to examine which regions of the promoter drive wild-type expression of *caudal* (Eckert et al 2004). Our collaborators are repeating this process for the *even-skipped* gene. These experiments are part of a larger project to characterize the promoter regions of *caudal* and *even-skipped* in order to understand how the segmentation clock is regulated at different stages of segmentation in *Tribolium*. In future experiments, we will utilize comparative RNA sequencing in staged *Tribolium* in order to identify possible

transcription factors for the *caudal* and *even-skipped* genes. This is the first attempt to define promoter regions in *Tribolium* and as such is a crucial step in dissecting regulatory inputs of the first model of a segmentation clock in arthropods.

The differences in the rate of the clock are correlated to diffences in the degree of cell movement: during the (18–20 hr) period of rapid segment addition germband elongation is driven by extensive cell rearrangements (Nakamoto et al. 2015). However, cells must maintain a continuous band of gene expression while undergoing extensive rearrangements. With a fate map of the blastoderm, we also hoped to address whether the initial clock output was stably maintained through cell rearrangements or the degree to which individual cells gained and lost eve expression.

The implications of this study go beyond merely predicting the segmental fates of sequentially segmenting insects. With a fate map of the blastoderm in *Tribolium* we can draw larger predictions about sequentially segmenting in arthropods, the most specious phylum, potentially revealing how much diversity in developmental mechanisms might be masked by our short-intermediate-long characterization.

Appendix

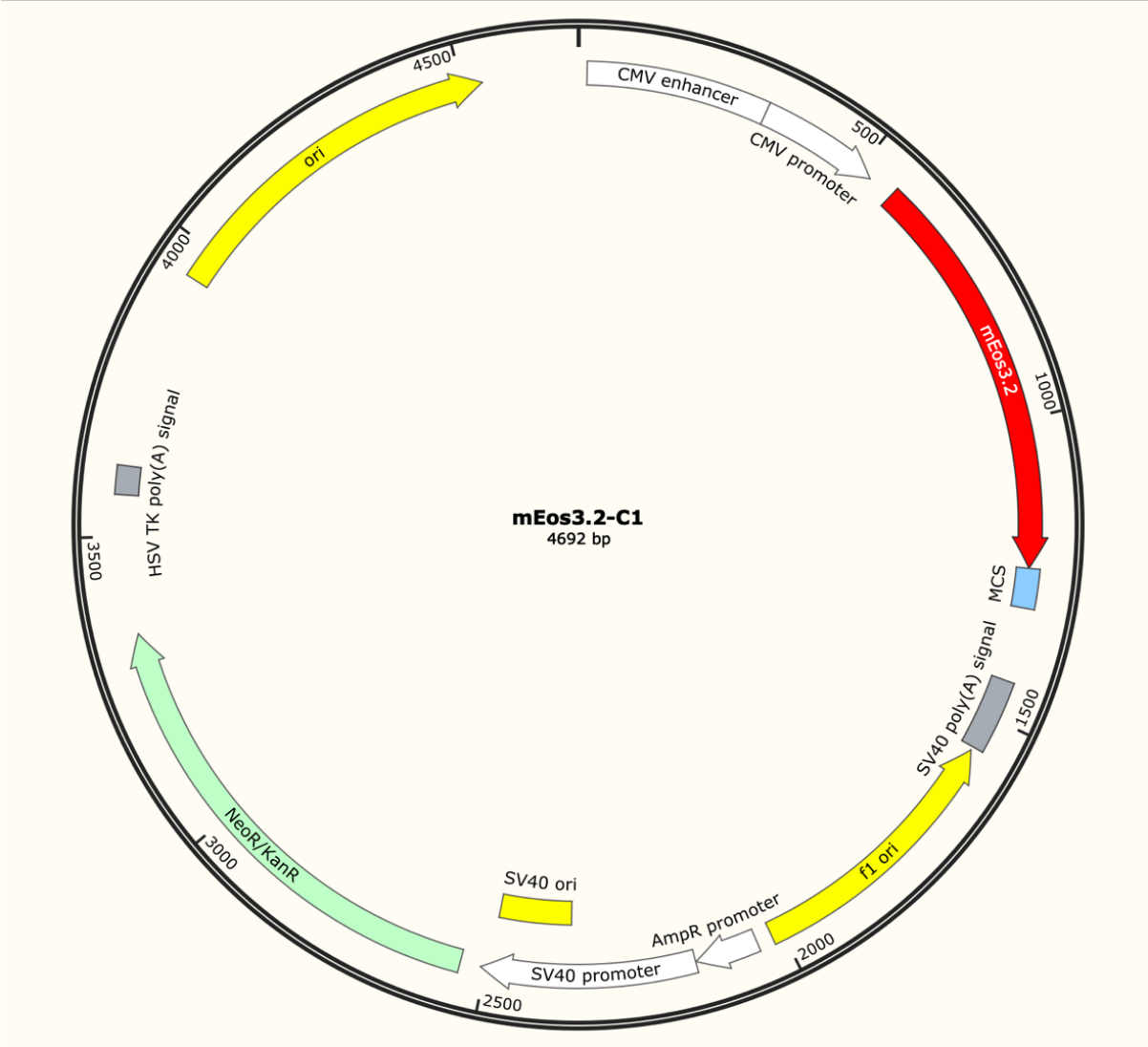

Image 1: mEos3.2-C1 plasmid. Plasmid has a CMVd1 promoter, EosFP and SV40 poly (A) tail. Eos is a photoconvertible dye. SV40 poly (A) tail is required for mRNA synthesis.

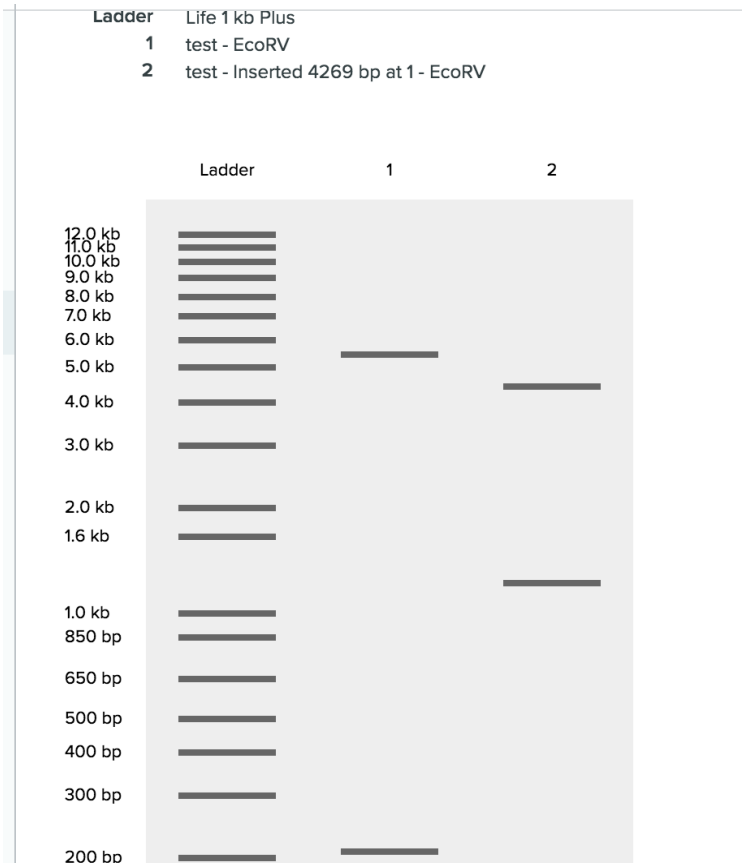

Image 2: *Eco*RV digest prediction. Lane 1 corresponds to the T7-Nls-Eos and Lane 2 corresponds to T3-Nls-Eos.

Literature Cited

Akam, M. 1987. The molecular basis for metameric pattern in the Drosophila embryo. Development **101**(1): 1.

Benton, M.A., and Pavlopoulos, A. 2014. Tribolium embryo morphogenesis. Bioarchitecture **4**(1): 16–21. doi:10.4161/bioa.27815.

Benton, M.A. 2018. A revised understanding of Tribolium morphogenesis further reconciles short and long germ development. PLOS Biol. **16**(7): e2005093. doi: 10.1371/journal.pbio.2005093.

Brown, A., Brown, S., Ellisor, D., Hagan, N., Normand, E., and Zervas, M. 2009. A Practical Approach to Genetic Inducible Fate Mapping: A Visual Guide to Mark and Track Cells In Vivo. J. Vis. Exp. (34). doi:10.3791/1687.

Campos-Ortega, J.A., and Hartenstein, V. 2014. The Embryonic Development of Drosophila melanogaster. *In*2. ed., Softcover reprint of the hardcover 2. ed. 1997. Berlin [u.a.] Springer.

Choe, C.P., Miller, S.C., and Brown, S.J. 2006. A pair-rule gene circuit defines segments sequentially in the short-germ insect Tribolium castaneum. Proc. Natl. Acad. Sci. U. S. A. **103**(17): 6560–6564. doi:10.1073/pnas.0510440103.

Damen, W.G.M. 2007. Evolutionary conservation and divergence of the segmentation process in arthropods. Dev. Dyn. Off. Publ. Am. Assoc. Anat. **236**(6): 1379–1391. doi:10.1002/dvdy.21157

Davis, G.K., and Patel, N.H. 2002. Short, Long, and Beyond: Molecular and Embryological Approaches to Insect Segmentation. Annu. Rev. Entomol. **47**(1): 669–699. doi: 10.1146/annurev.ento.47.091201.145251.

El-Sherif, E., Averof, M., and Brown, S.J. 2012. A segmentation clock operating in blastoderm and germband stages of Tribolium development. Dev. Camb. Engl. **139**(23): 4341–4346. doi:10.1242/dev.085126.

Fortey, R.A., and Thomas, R.H. 1997. Arthropod Relationships. Springer Science & Business Media.

Gilbert, S.F. 2000. The Origins of Anterior-Posterior Polarity. Dev. Biol. 6th Ed.

Gilbert, Scott F. and Michael J. F. Barresi. 2016. *Developmental Biology*. Eleventh ed. Sunderland, Massachusetts: Sinauer Associates.

Golomb, M., and Chamberlin, M.J. 1977. T7- and T3-Specific RNA Polymerases: Characterization and Mapping of the In Vitro Transcripts Read from T3 DNA. J VIROL **21**: 10.

Handel, K., Grünfelder, C.G., Roth, S., and Sander, K. 2000. Tribolium embryogenesis: a SEM study of cell shapes and movements from blastoderm to serosal closure. Dev. Genes Evol. **210**(4): 167–179. doi:10.1007/s004270050301.

Hsu, Y.-C. 2015. The Theory and Practice of Lineage Tracing. Stem Cells Dayt. Ohio **33**(11): 3197–3204. doi:10.1002/stem.2123.

Klement, J.F., Moorefield, M.B., Jorgensen, E., Brown, J.E., Risman, S., and McAllister, W.T. 1990. Discrimination between bacteriophage T3 and T7 promoters by the T3 and T7 RNA polymerases depends primarily upon a three base-pair region located 10 to 12 base-pairs upstream from the start site. J. Mol. Biol. **215**(1): 21–29.

Liao BK and Oates AC. 2017. Delta-Notch signalling in segmentation. Arthropod Struct. Dev. **46(3):**429-447. doi: 10.1016/j.asd.2016.11.007.

Liu, P.Z., and Kaufman, T.C. 2005. Short and long germ segmentation: unanswered questions in the evolution of a developmental mode. Evol. & Dev. **7**(6): 629–646. doi:10.1111/j.1525-142X.2005.05066.x.

Lohs-schardin, M., and Cremer, C. 1979. A fate map for the larval epidermis of Drosophila melanogaster: localized cuticle defects following irradiation of the blastoderm with an ultraviolet microbeam.

Nakamoto, A., Hester, S.D., Constantinou, S.J., Blaine, W.G., Tewksbury, A.B., Matei, M.T., Nagy, L.M., and Williams, T.A. 2015. Changing cell behaviours during beetle embryogenesis correlates with slowing of segmentation. Nat. Commun. **6**: 6635. doi:10.1038/ncomms7635.

Nüsslein-Volhard, C., and Wieschaus, E. 1980. Mutations affecting segment number and polarity in Drosophila. Nature **287**(5785): 795–801. doi:10.1038/287795a0.

Pourquie, O. 2001. The vertebrate segmentation clock. J. Anat. **199**(Pt 1-2): 169–175.

Sander, K. 1994. The evolution of insect patterning mechanisms: a survey of progress and problems in comparative molecular embryology. : 5.

Sander, K. 1996. Pattern formation in insect embryogenesis: The evolution of concepts and mechanisms. Int. J. Insect Morphol. Embryol. **25**(4): 349–367. doi:10.1016/S0020-7322(96)00021-9.

Sarrazin, A.F., Peel, A.D., and Averof, M. 2012. A segmentation clock with two-segment periodicity in insects. Science **336**(6079): 338–341. doi:10.1126/science.1218256

Schmidt-Ott, U., Gonzalez-Gaitan, M., Jackle, H., and Technau, G.M. 1994. Number, identity, and sequence of the Drosophila head segments as revealed by neural elements and their deletion patterns in mutants. Proc. Natl. Acad. Sci. **91**(18): 8363–8367. doi:10.1073/pnas.91.18.8363.

Tang, G.-Q., Bandwar, R.P., and Patel, S.S. 2005. Extended Upstream A-T Sequence Increases T7 Promoter Strength. J. Biol. Chem. **280**(49): 40707–40713. doi:10.1074/jbc.M508013200

Tautz, D., Friedrich, M., and Schröder, R. (n.d.). Insect embryogenesis – what is ancestral and what is derived? : 7.

Wang, L., Wang, S., Li, Y., Paradesi, M.S.R., and Brown, S.J. 2007. BeetleBase: the model organism database for Tribolium castaneum. Nucleic Acids Res. **35**(Database issue): D476–D479. doi:10.1093/nar/gkl776

Wang, J., Du, Y., Wang, S., Brown, S.J., and Park, Y. 2008. Large diversity of the piggyBac-like elements in the genome of Tribolium castaneum. Insect Biochem. Mol. Biol. **38**(4): 490–498. doi: 10.1016/j.ibmb.2007.04.012.

Wiedenmann, J., Ivanchenko, S., Oswald, F., Schmitt, F., Röcker, C., Salih, A., Spindler, K.-D., and Nienhaus, G.U. 2004. EosFP, a fluorescent marker protein with UV-inducible green-to-red fluorescence conversion. Proc. Natl. Acad. Sci. **101**(45): 15905–15910. doi:10.1073/pnas.0403668101.

Williams, Terri A. and Nagy, Lisa M. 2016. Linking gene regulation to cell behaviors in the posterior growth zone of sequentially segmenting arthropods. Arthropod Struct Dev. 2016 Oct 5. pii: S1467-8039(16)30146-3. doi: 10.1016/j.asd.2016.10.003